III. PLASMA DYNAMICS

Prof. S. C. Brown   Prof. H. H. Woodson   A. T. Lewis
Prof. O. K. Mawardi   D. A. East   Z. J. J. Stekly

A. HYDROMAGNETIC WAVEGUIDE

The purpose of this investigation is to study the dynamics of wave propagation in a hydromagnetic waveguide. This waveguide consists of an electrically conducting conduit inserted in the field of a steady magnetic field, and it is assumed to be filled with plasma. Suppose, for the simplest case, that the applied field is parallel to the axis of the tube. When the plasma moves with a fluctuating velocity in a direction normal to the axis of the waveguide, the lines of force are shaken to and fro in the direction of the applied velocity. A transverse wave is thereby made to travel along the lines of force. More complex situations will also be discussed.

It is well known to workers in hydromagnetics that the governing relations for the motion of a plasma in a magnetic field are analogous to those describing the behavior of an ideally conducting fluid in the presence of a magnetic field. Hence, our discussion begins with the relations for the conservation of momentum and matter and with the equation of state. As a result of linearization, we find that these equations are

$$\rho_o \frac{\partial \vec{v}}{\partial t} = - \nabla p + \vec{j} \times \vec{B}_o \tag{1}$$

$$\frac{\partial \rho}{\partial t} + \rho_o \nabla \cdot \vec{v} = 0 \tag{2}$$

$$p = a^2 \rho \tag{3}$$

In these expressions, zero subscripts indicate quiescent values, and lower-case letters fluctuating variables. The velocity is denoted by $\vec{v}$, the pressure by p, the density by ρ, the velocity of sound waves in free space by a, the fluctuating local current density by $\vec{j}$, and the applied steady magnetic field by $\vec{B}_o$.

The set of corresponding Maxwellian relations, corrected for relativistic effects, is

$$\nabla \times \vec{e} = - \frac{\partial \vec{b}}{\partial t} \tag{4}$$

$$\nabla \times \vec{b} = \mu \vec{j} \tag{5}$$

$$\vec{e} + \vec{v} \times \vec{B}_o = 0 \tag{6}$$

The fluctuating magnetic field is denoted by $\vec{b}$, the electric field by $\vec{e}$, and the permeability of the medium by μ. Relations 4, 5, and 6 are valid when the plasma is quasineutral, and when the characteristic dimension of the apparatus is large compared with both the

mean free path of the gas and the Debye shielding distance.

It can be readily found that the velocity satisfies the equation

$$k^2 \vec{v} + \beta^2 \, \nabla(\nabla \cdot \vec{v}) + [\nabla \times \nabla \times (\vec{v} \times \vec{i}_b)] \times \vec{i}_b = 0 \tag{7}$$

in which $k = \omega/c$, the wave number for the Alfvén wave velocity in free space. This velocity c equals $B_o/(\mu\rho)^{1/2}$. The parameter $\beta = a/c$ is the ratio of the two velocities of wave propagation, and $\vec{i}_b$ indicates a unit vector in the direction of the magnetic field. Similar relations for the other field variables can be obtained by manipulating the set of Eqs. 1-6. The appropriate boundary conditions for the problem require the vanishing of the normal components of the oscillating velocity and the magnetic field at the walls of the waveguide. If we define the velocity by the identity

$$\vec{v} = \nabla\phi + \nabla \times \vec{M} \tag{8}$$

it can be shown by substituting Eq. 8 in Eq. 7 that we obtain two simultaneous equations in the velocity potentials ϕ and $\vec{M}$. These equations for the general case, when $\vec{i}_b$ is at an arbitrary angle with the axis of the waveguide, are quite complicated and have to be solved approximately. Two extreme cases, however, allow the equations to be solved exactly. The results for these two cases will now be briefly indicated.

Case 1. The magnetic field is aligned with the axis of the waveguide. Then the two wave modes propagate along the axis of the waveguide. One of these modes displays the character of a longitudinal, or compressive, wave and is called, in this report, the "acoustic wave." The other mode is of transverse character and represents the hydromagnetic mode. Several interesting alternatives may occur that depend upon whether β is less than or greater than unity.

When β is less than unity, the acoustic mode has no cutoff for all orders of the wave eigen numbers. This is quite different from the conventional acoustic wave propagation that takes place in a pipe. The hydromagnetic mode does, however, have a cutoff that depends upon the order of the eigen number. It can be checked that whenever $\beta < 1$, the pressure from collisions, p, is considerably lower than the hydromagnetic pressure $B_o/2\mu$. This means, of course, that the collective behavior of the electrons is controlled, in large part, by the electromagnetic forces. When $\beta > 1$, we find that the hydromagnetic mode is then the mode that suffers no cutoff for all orders of the wave eigen number. The acoustic mode, on the other hand, has a cutoff frequency that depends on the order of the wave eigen number. The case of $\beta > 1$ indicates that the density of the plasma is high, and is probably more representative of the density of a liquid metal than of the density of a plasma.

An interpretation of the reversal of the noncutoff property of the two waves for $\beta \lessgtr 1$ can be given by visualizing the behavior of the plasma as it is squeezed by the

lines of forces during their transverse motion. For stronger magnetic forces with $\beta < 1$, a side distortion of the lines is always accompanied by a longitudinal forward motion of the plasma, hence the acoustic wave suffers no cutoff. A similar explanation can be given for the behavior with $\beta > 1$.

The expression for the component of the velocity transverse to the axis of the wave-guide is given by

$$v_x = (1 + \kappa^2)\, e^{i\kappa|y|} \frac{(2n + 1)\pi}{2L_1} \cos \frac{(2n + 1)\pi x}{2L_1} \sin \frac{(2m + 1)\pi z}{2L_2} \tag{9}$$

$$v_z = (1 + \kappa^2)\, e^{i\kappa|y|} \frac{(2m + 1)\pi}{2L_2} \sin \frac{(2n + 1)\pi x}{2L_1} \cos \frac{(2m + 1)\pi z}{2L_2} \tag{10}$$

in which n, m = 0, ±1, ±2, ...; and $2L_1$ $2L_2$ are the width and height of the waveguide section. In expressions 9 and 10, κ is the propagation constant for the waves. The functional relation of κ on k, the wave number, is shown in graphical form in Fig. III-1 for $\beta \lessgtr 1$ and $\beta = 1$.

It is obvious that for $\beta = 1$, it is not possible to identify the particular wave associated
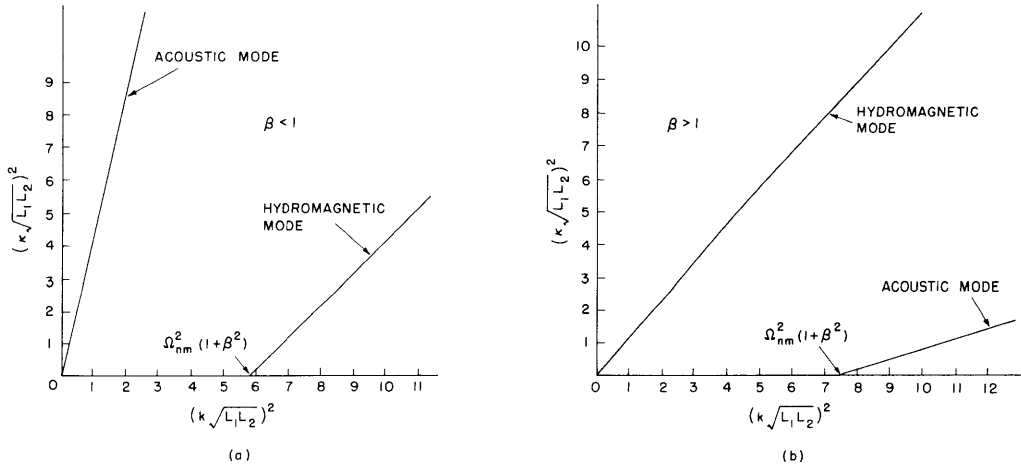

Fig. III-1. Dependence of the propagation constant on the frequency.
(a) The cutoff for the hydromagnetic mode is given as a function of

$$\Omega^2_{mn} = \frac{\pi^2}{4}\left(\frac{(2n + 1)^2 L_2}{L_1} + \frac{(2m + 1)^2 L_2}{L_2}\right).$$

(b) The cutoff for the acoustic mode is given as a function of

$$\Omega^2_{mn} = \frac{\pi^2}{4}\left(\frac{(2n + 1)^2 L_2}{L_1} + \frac{(2m + 1)^2 L_1}{L_2}\right).$$

with the two branches of the function $\kappa = f(k)$.

Case 2. The magnetic field direction is at right angles to the axis of the waveguide. In this case, the analysis shows that no hydromagnetic wave propagates along the axis of the waveguide. Indeed, consideration of this situation leads us to conclude that the hydromagnetic wave appears as a standing wave along the lines of force, and hence it is trapped between the walls of the waveguide.

The alignment of the magnetic field in another direction besides the two that have been mentioned gives rise to intermediate situations which, however, cannot be obtained as a superposition of the two waves indicated in Eqs. 1 and 2 because Eq. 7 is not linear in the vector $\vec{i}_b$.

The analysis that has been given cannot be extended to frequencies higher than the ion cyclotron frequency, without taking into account the necessary correction, because the plasma is now composed of two fluids interacting with the magnetic field. This correction is easily made, and it can be shown that the symmetry of the eigenfunctions in the positive and negative values is lost.

Work is now being done to check these speculations experimentally.

O. K. Mawardi

B. HYDROMAGNETIC INSTABILITIES

A series of investigations has been started to study the onset and the growth rate of the instability in a cylinder of plasma under different conditions. In the preliminary experimental phase, the work will be done on liquid metals.

The situation that has just been investigated is concerned with an instability similar to that produced by the "pinch effect." Here, however, the electromagnetic forces are
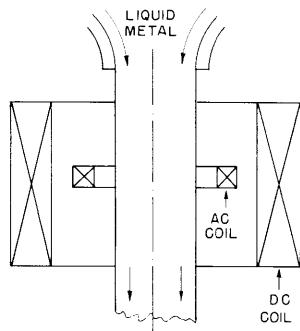

Fig. III-2. Schematic representation of apparatus used to study instabilities.

caused by the interaction of an applied steady magnetic field parallel and external to a column of fluid with azimuthal currents induced in the column. The column with free surfaces is simulated by allowing liquid metal to fall unimpeded from a reservoir. The

forced current is induced by a coil that is coaxial to the column, as illustrated in Fig. III-2.

The theoretical prediction for the dynamical behavior of the column is being studied by means of a normal-mode technique.

O. K. Mawardi, D. A. East

C. STUDIES OF MAGNETOHYDRODYNAMIC SHOCKS

The work reported here was started for the purpose of investigating the dynamics and the structure of hydromagnetic shocks. In particular, the parameters of the shock that have to be estimated are its thickness, pressure ratio, magnetic-field ratio, and the corresponding density ratio. The preliminary theoretical work was carried out on the basis of a continuum theory.

The calculations follow conventional techniques for studies on shock waves, i.e., the discussion begins with the equation for the conservation of momentum and mass. An appropriate equation of state is also introduced. The hydromagnetic interaction is taken into account by means of a well-known relation for the magnetic field,

$$\frac{\partial \vec{H}}{\partial t} = \nabla \times (\vec{v} \times \vec{H}) - \frac{1}{\mu\sigma} \nabla^2 \vec{H} \tag{1}$$

where $\vec{H}$ is the intensity of the magnetic field, $\vec{v}$ is the velocity, μ is the permeability, and σ is the conductivity.

It can be shown that a one-dimensional dependence for the variables leads to expressions 2 and 3 which relate the value of the upstream parameters of the shock to its downstream parameters. The relations are valid for distances that are large compared with the thickness of the shock. Manipulation of all of the equations mentioned in Sec. III-A leads to a pair of simultaneous expressions, the first of which is

$$\frac{\beta_1^2}{\beta_0^2} = \frac{1 + \left(\frac{1}{2} + M_1^2\right)\gamma\beta_1^2}{1 + \left(\frac{1}{2} + M_0^2\right)\gamma\beta_0^2} \tag{2}$$

The symbol

$$\beta_{o,1}^2 = \left(\frac{\mu H_{o,1}^2}{\rho_{o,1}}\right) \Big/ \left(\frac{\gamma P_{o,1}}{\rho_{o,1}}\right)$$

stands for the ratio of the square of the Alfvén velocity to the square of the velocity of sound; $M_{o,1}$ is the appropriate hydromagnetic Mach number, defined as the ratio of the local velocity to the Alfvén velocity.

For the second relation, we have

27

$$\frac{\beta_1^2}{\beta_0^2} = \frac{1 + \frac{(\gamma-1)}{2} \beta_1^2 \left(M_1^2 + 2\right)}{1 + \frac{(\gamma-1)}{2} \beta_0^2 \left(M_0^2 + 2\right)} \tag{3}$$

Equations 2 and 3 are sufficient to define completely the state of the gas downstream of the shock.

The experimental verification of this discussion will be carried out by means of an apparatus that will allow a magnetically driven shock to travel in an externally applied uniform magnetic field. This apparatus is now being constructed.

O. K. Mawardi, Z. J. J. Stekly

D. CONSTRUCTION AND INSTRUMENTATION OF A T TUBE FOR MAGNETICALLY DRIVEN SHOCKS

A T tube with a backstrap for magnetic driving of a shock has been constructed and is in operation. The tube is of conventional design, as illustrated in Fig. III-3. The immediate purpose of this tube is to reproduce results of earlier workers (1, 2, 3) in this field so that instrumentation can be checked and perfected.
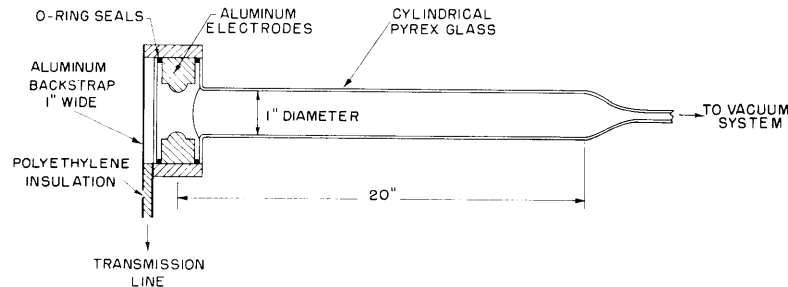

Fig. III-3. T tube construction.

The transmission line passes through a triggered spark-gap switch to a 2.5-μfd capacitor bank. A 5-kv power supply is being used, but a 35-kv power supply is available and it will be used to reach voltages higher than 5 kv. Tank hydrogen at pressures in the range 1-2 mm Hg is used in the tube. The current waveform has been observed, both conductively and inductively, and it is characterized by an underdamped oscillation, the frequency of which is 250 kcps, and of damping in which the oscillations decrease by a factor of 3/5 per cycle. The current amplitude is measured by a calibrated shunt.

Photomultiplier circuitry is being assembled so that three tubes will be available for measuring the average velocity of the luminous front. Data obtained from a single 1P28 photomultiplier tube, located 10 cm from the spark, show an abrupt rise in light intensity 3 μsec after initial breakdown of the gap when the hydrogen pressure is 0.7 mm Hg, and the voltage is 5000 volts. The observed waveform is shown in Fig. III-4. The initial peak is caused by stray pickup of the capacitor discharge. The peak at approximately 15 μsec may arise from a shock reflected from the wall just in front of the backstrap. These are only preliminary results; however, the sudden increase in light intensity at 3 μsec indicates that a fairly strong shock has formed in the gas and is propagating at an average speed of approximately 3 cm/μsec.
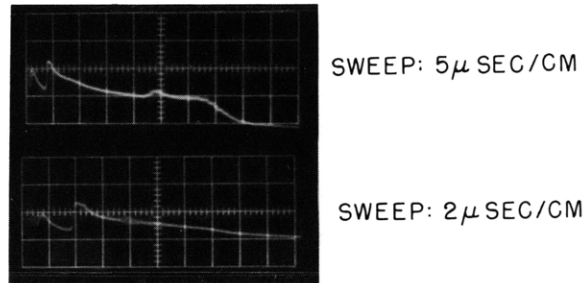
SWEEP: 5μ SEC/CM

SWEEP: 2μ SEC/CM

Fig. III-4. Oscillogram showing the response of a 1P28 photomultiplier tube at 10 cm from the discharge. A 2.5-μfd capacitor bank at 5000 volts is discharged into hydrogen gas at a pressure of 0.7 mm Hg. The oscilloscope is triggered by the time rate of change of the arc current.

The picture taken with a slow sweep shows a light output of approximately 40 μsec duration. Photoexcitation of the gas by the light from the initial arc and excitation from incident and reflected shock waves offer the most logical explanation for this. The relaxation time for the gas that is excited in this manner is of the correct order of magnitude for explaining the observed phenomenon. An instrumentation apparatus has been perfected for measuring the properties of that part of the gas with only ordered motion.

The pressure in the tube before the discharge of the capacitor bank is measured by a thermocouple gauge at pressures lower than 1 mm Hg, and a mercury-filled manometer is used at higher pressures. Unfortunately, both of these devices are inaccurate in the vicinity of 1 mm Hg pressure; consequently, improved pressure-measuring apparatus will have to be assembled.

Some difficulty was experienced, initially, in photographing the single-shot sweeps

obtained from the experimental apparatus. At present, Polaroid Type 44 film (Polapan 400) produces adequate pictures down to a sweep rate of 1 cm/μsec with a P-11 tube phosphor and with the 10,000-volt accelerating potential of the oscilloscope (Tektronix Model 541 with a 53/54-k plug-in amplifier).

<div align="right">A. T. Lewis, H. H. Woodson</div>

References

1. R. G. Fowler, J. S. Goldstein, and Beryl E. Clotfelter, Luminous fronts in pulsed gas discharges, Phys. Rev. 82, 879 (1951).

2. R. G. Fowler, W. R. Atkinson, and L. W. Marks, Ion concentrations and recombinations in expanding low pressure sparks, Phys. Rev. 87, 966 (1952).

3. A. C. Kolb, Production of high-energy plasmas by magnetically driven shock waves, Phys. Rev. 107, 345 (1957).